

## Effect of Soft-hard Plate and Rubber Sandwich Against on 5.56 mm Deformable Projectile

Helmy Purwanto<sup>1,2,\*</sup>, Rudy Soenoko<sup>3</sup>, Anindito Purnowidodo<sup>3</sup> and Agus Suprpto<sup>4</sup>

<sup>1</sup> Department of Mechanical Engineering, Wahid Hasyim University, Semarang, Indonesia

<sup>2</sup> Doctoral Student in Department of Mechanical Engineering, Brawijaya University, Malang, Indonesia

<sup>3</sup> Department of Mechanical Engineering, Brawijaya University, Malang, Indonesia

<sup>4</sup> Department of Mechanical Engineering, Merdeka University, Malang, Indonesia

Received 8 August 2017; Accepted 15 September 2017

### Abstract

In this paper, the effect of soft-hard plate and rubber thickness as absorbent impact against on ballistic resistance with 5.56 x 45 mm caliber deformable projectile is investigated. The characteristic of ballistic impact for each configuration target is obtained and compared based on the investigation of the hardness effect of the front plate and the thickness of rubber. The experimental results approached by simulation with finite element method were used to know several characters due to the ballistic impact. The experiment and simulation results showed that the projectile is able to perforate front plate and the impact on the back plate form a bulge on every configuration. The configuration of hard plate as front plate reveals minimum ballistic impact due to the projectile rate. The simulation shows that the maximum stress concentration occurs only on the front plate, so the front plate fails.

Keywords: Sandwich plate, rubber, impact characteristic, experiment, simulation

### 1. Introduction

The design of military vehicles is very concerned about the dynamics of performance when moving and/or firing [1] other than the material used for the stability and efficiency. Military vehicles have long used steel plate body armor as protection against ballistic attack. The attack modes on armor are broadly classified to kinetic energy attack, momentum attack, shockwave attack, and diffused pressure pulse attack [2]. Armor used in military vehicles is usually monolithic high strength metal plate with a certain thickness to protect ballistic attack; the use of multi-layered plate is developed because the expected thickness is not always manufactured and meet the design specifications [3].

Materials selection in multi-layer ceramic composite armor influences the character of a ballistic impact. Material on the third layer (carbon fiber plate and aluminum alloy) in the composite back plates, Ti6Al4V provides a strong supporting role to the first layer and simultaneously enhance the energy balance function from the middle layer of UHMWPE [4]. The first layer has a function to absorb the kinetic energy of a bullet, its destabilization, deflection and deformation, whereas the next layer absorbs the remaining kinetic energy of the deformed and/or fragmented projectile [5].

The results of studies on the monolithic and double-layered target using blunt and ogival projectiles in an experimental and simulation showed ballistic limit velocity. The minimum ballistic limit velocity obtained by independent projectile nose shape seemed to increase

significantly by double-layering the target [6]. Yunfei et al. [7] had also been conducting experiments of ballistic performance with blunt and ogival-nosed projectiles of double-layered steel plates of different materials. Result showed that the double-layered plates of the upper layer with high strength and low ductility material and the lower layer of low strength and high ductility have higher ballistic limit velocities than the configuration of the opposite layering order. The ogival-nosed projectiles were significantly smaller than those of blunt nosed projectiles ballistic limit velocities. Perforation mechanisms and failure modes of plates and projectiles caused differences in the ballistic limit velocities [8], and the ballistic resistance of multi-layered target affected by order of layers, the multi-layered targets of two equal thick plates have the highest ballistic resistance compared to different thick plates [9].

Teng et al., [10] evaluated the effect of projectile with different nose shape and weight shot on monolithic and double-layered plate by using the finite element method. The result of the simulation showed that the double-layered plate was more ballistic resistant 8.0%–25.0 % for the flat-nose projectile, compared to the monolithic plate of the same weight. Teng et al., [11] in his other study, also reported that plate configuration with high ductility-low strength in the front plate with low ductility-high strength in back plate was the best, the configuration result was 25% in the ballistic limit.

Pechoucek [12] conducted experiments and simulation using high strength steel to assess ballistic efficiency of some layered structures. Materials used were steel, ceramics, concrete and some ductile materials. The results demonstrated the ability of layered plates to withstand projectiles at level 3 and 5 STANAG 4569 standard.

\*E-mail address: [helmypurwanto@unwahid.ac.id](mailto:helmypurwanto@unwahid.ac.id)

ISSN: 1791-2377 © 2018. Eastern Macedonia and Thrace Institute of Technology. All rights reserved.

doi:10.25103/jestr.111.06

Meanwhile, Wei et al. [13] investigated the ballistic performance of multi-layered metal plates subjected by providing an air gap to impact by blunt rigid projectiles. The result showed that layered targets with larger air gap were stronger than those with small air gap. Ballistic failures on high strength plates as well influenced by angle of attack, the angle of attack perpendicular to the plate can penetrate the plate with a hole diameter larger than the projectile caliber [14].

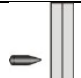
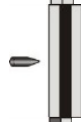


Rubber is a material that can absorb impact energy. Natural or artificial elastomer can be used as a material in the composite to increase the impact toughness [15]. Polyuria coating indicates a good ability in absorbing energy and reduction of the residual velocity of the projectiles [16]. Impact angle on steel/rubber/composite hybrid structure shows a stronger effect with increasing plastic deformation and dissipated energy compared to the projectile velocity number of impacts, sample temperature, and prior aging used [17]. Elastomer coating on the surface of the hard steel plate may delocalize the impact stress; thus it contributes to a higher ballistic limit [18], reduces the pressure so that the penetration resistance increases [19]. Yunfei et al. [7] also revealed that perforation at the localized mechanism and perforation process with overall structural deformation interaction is an important aspect in analyzing the multi-layered plate problem.

Studies to compare between monolithic/single plat with layered/sandwich plate using several plates with the same total thickness and manufactured from the same material and different materials have been many reported [5][6][9][10][11][13], but the one which focuses on manufacturing to one plate that has the free (non-fixed) and the use of rubber as absorbers is slightly reported. This study aims to observe and investigate the macrostructure sandwich plate (soft and hard-plate with rubber) in which the two plates are manufactured non-fixed due to projectile impact.

## 2. Experimental Procedure

Sandwich plates made of a soft plate, hard plate, and rubber as ballistic panels with the configuration see Tab. 1. Mechanical properties steel plate and rubber see Tab. 2. Standard test method for Brinell hardness of metallic materials with ASTM E10, tension testing of metallic materials with ASTM E8, and notched bar impact testing of metallic materials use ASTM E23. While Standard test hardness for rubber uses Indonesian standard SNI 0778:2009; tensile stress-strain properties for rubber use ISO 37:2011, tear strength for rubber uses ISO 34-1:2010 and determination of compression set uses ISO 815-1:2014.

**Table 1.** Sandwich plate configurations

Configuration	Geometry	Thickness	Code
Soft-soft plate		6 mm soft plate - 6 mm back plate	S.0
Soft-rubber-soft plate		6 mm soft plate - 2 mm rubber - 6 mm back plate	S.2
		6 mm soft plate - 4 mm rubber - 6 mm back plate	S.4
		6 mm soft plate - 6 mm rubber - 6 mm back plate	S.6
Hard-soft plate		6 mm hard plate - 6 mm back plate	H.0
Hard-rubber-soft plate		6 mm hard plate - 2 mm rubber - 6 mm back plate	H.2
		6 mm hard plate - 4 mm rubber - 6 mm back plate	H.4
		6 mm hard plate - 6 mm rubber - 6 mm back plate	H.6

**Table 2.** The average mechanical properties of materials

Material	Hardnes	Max Stress (MPa)	$\epsilon$ (%)	Impact Energy (J)	Tear strength (N/mm)	Determination of compressions (%)
Soft plate/back plate	118.21 BHN	458.16	31	62.48	-	-
Hard plate	478.23 BHN	1466.19	13	47.77	-	-
Rubber	67 Shore A	4.21	120	-	2.08	34.01

The back plate which used soft plate was fixed in the holder ballistic tests while the front plate was made non-fixed to make a hole clearance toward the bolts for binder configuration. Manufactured sandwich plates see Fig. 1a, while scheme ballistic testing is shown in Fig. 1b. Ballistic testing performed for each configuration using 5.56 x 45 mm M-193 deformed full metal jacket projectile is shown in Fig. 2a. Projectile fired with normal angle of attack at the shooting range of 15 m with the average velocity of 989 m/s was measured using a chronograph. Ballistic impact on the plate was observed and measured to determine the characteristics of the impact on each

configuration. Ballistic impact measurements on the front plate is  $I$ , back plate is  $II$ , and rubber is  $R$ . Hole diameter of front face is  $d_I$  (mm), hole diameter of inner side is  $d_2$  (mm), high of petal front face is  $p_I$  (mm), high of petal inner side is  $p_2$  (mm), front plate thickness is  $t_I$  (mm), back plate thickness is  $t_{II}$  (mm), rubber thickness is  $r$  (mm), depth of penetration in front plate is  $DoP_I$  (mm), depth of penetration in back plate is  $DoP_{II}$  (mm), and high of bulge is  $B$  (mm). The nomenclatures of dimensional measurement ballistic impact see Fig. 2b.

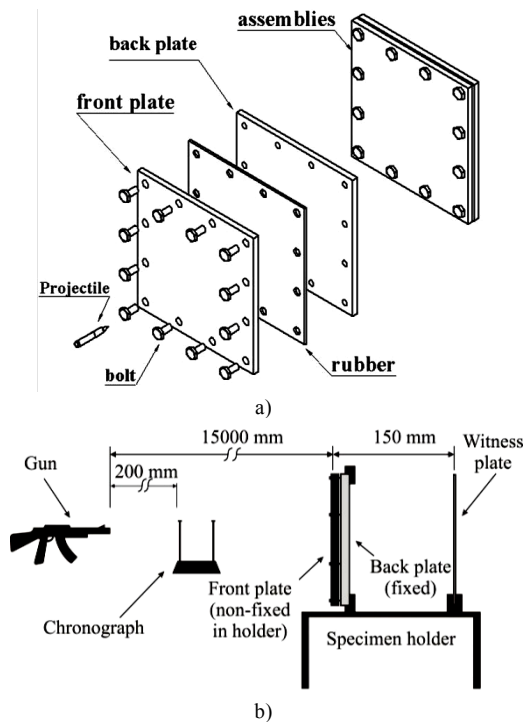


Fig. 1. (a). Manufactured sandwich plate, (b). Schematic view of ballistic test

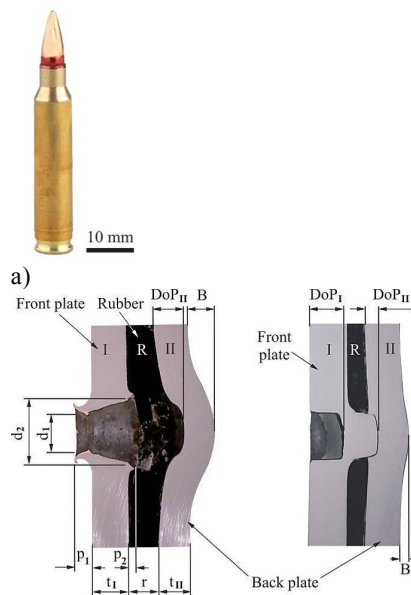


Fig. 2. (a). Projectile, (b). Nomenclature of dimensional measurement ballistic impact

Simulation is used to analyze the phenomenon of impact and some specific character in the plate target and projectile. The simulation based on finite element method with explicit dynamic in ANSYS code is used. Geometry and condition on the simulation are made similar as the experiment. The plate and projectile material are modeled as elastics-plastics material and the rubber is modeled as hyperplastic material. Fine meshing is 1 mm on the target and initial velocity of projectile is 989 m/s. Figure 3 shows simulation model and meshing of the specimen.

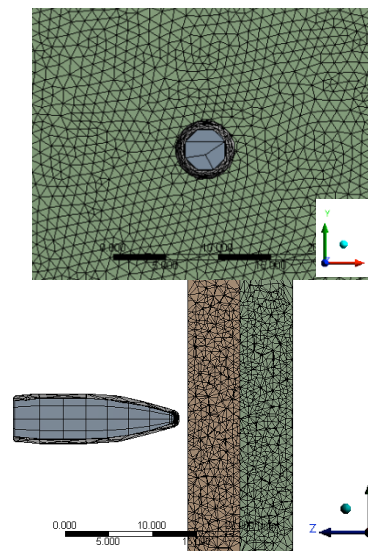


Fig. 3. Simulation model and meshing of the specimen

### 3. Result and Discussion

#### 3.1. Soft plate – soft plate (S.0)

The ballistic test result on S.0 sandwich plate configuration see Fig. 4. In this configuration, a projectile could penetrate front plate. Front plate in this configuration used soft plate. While the back plate that also used soft plate was impenetrable. Projectile could be penetrated and broke front plate and formed petals at the front face (Fig. 4a) and inner side plate (Fig. 4b). The edge of petal was yellowish due to projectile jacket made of brass attached. The residual velocity of the projectile and plate spall was still able to push the back plate; as a result, it deformed. Form of failure in the back plate was indicated by the shape of basin in the inside (Fig. 4b) and the bulge on the rear face (Fig. 4c). The dominant failure models of the front plate in this configuration were petalling and fragmentations, while on the back plate was bulging. The failure model of petalling is indicated by the formation of petals in front face and inner side on the front plate (Fig 4a. and Fig. 4b). The Failure models of fragmentation were indicated by the plate and projectile fragments found between the front plate – back plate and around the test area. Petalling models occurred on the low strength and high ductility plates. The plates are easily deformed plastic when there is a projectile impact with a pointed tip. Projectiles with pointed ends are capable of puncturing and deforming the plate. Although the projectile is made of soft material lead with a brass jacket, but in this case, the plate was more deformed than the projectile. Low strength on the plate caused the plate easily penetrated by a projectile although the high toughness and impact energy. The Plate was not able to withstand projectiles at high velocity with an ogival/tapered-nosed. High ductility on the plate caused the plate easily deformed thus forming petal on both the front face and back face in the first layer plate.

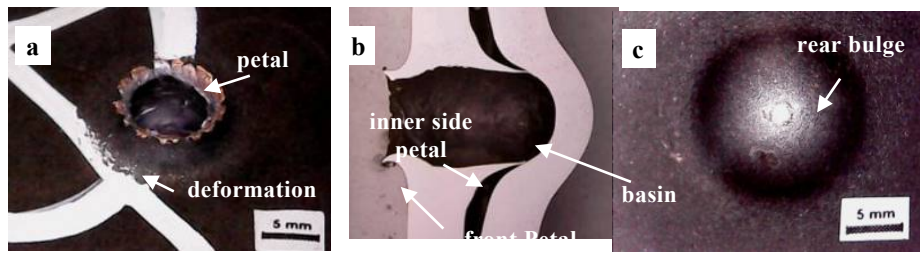


Fig. 4. Ballistic impact on the S.0 configuration (a) front face in front plate, (b) cross section, and (c) rear face in back plate

In the present study, simulation was used to know the penetration process of the projectile into the plates. The simulation to understand how is penetrating process of the projectile, the stress distribution and concentration, deformation process, and residual velocity of the projectile. Penetrating process of the projectile at time  $t$  (s) and residual velocity of projectile  $v$  (m/s) were analyzed. The

contour colors represent the stress distribution in which the red color indicates the highest region of stress concentration (MPa). The stress concentration becomes lower in the region on which the red color shifts gradually to the blue one. Stress distribution and concentration, deformation, petalling and penetrating processes in the sandwich plate S.0 configuration see Fig. 5.

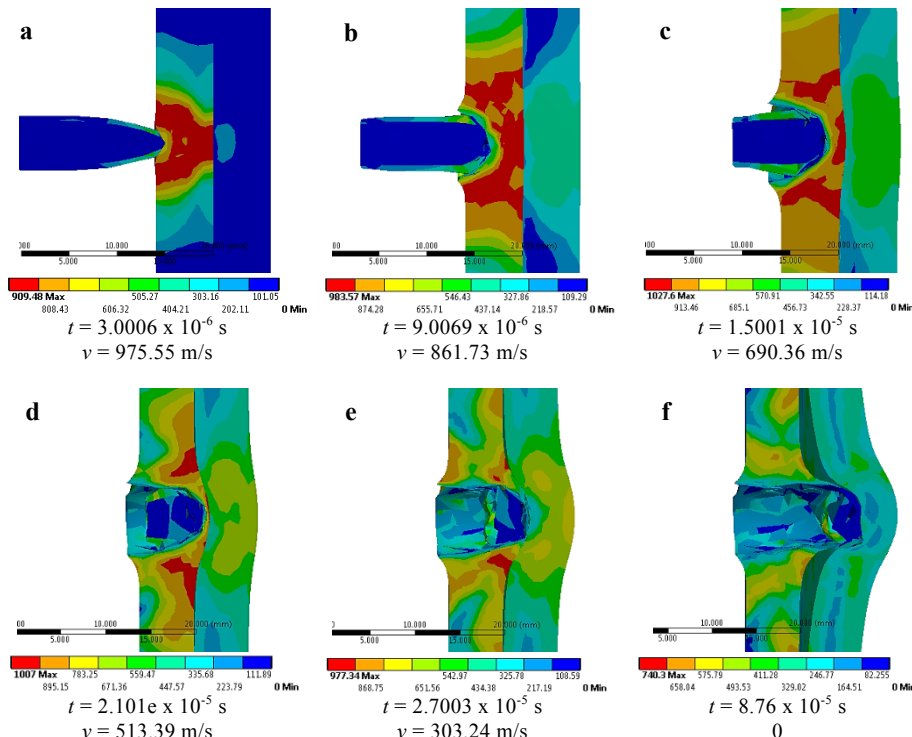


Fig. 5. Impact process of projectile on plate S.0 configuration (equivalent stress-von misses)

The Fig. 5 shows that the tip of the projectile hit to front plate, so the plate got a maximum stress concentration at around radius of projectile (Fig. 5a). Because the maximum stress concentration occurred at the plate surface, the projectiles were capable of piercing front plate by deforming and breaking it. Afterwards, projectile pierced the front plate, so plate and projectile began to deform. The pointed end of the projectile began to blunt, while the plate began to deform and form the petals on the front face (Fig. 5b). The greater projectile deformation, the greater the hole formed on the front plate would be (Fig. 5c). Maximum stress concentration indicated by red color was still visible, so the projectile could still pierce the plate and penetrate the front plate (Fig. 5d and Fig. 5e). The stress that occurred at the plate increased due to the impact force of projectile (Fig. 5a – Fig. 5c) until it reached the maximum stress at 1027.60 MPa. The stress went gradually down after reaching its maximum value (Fig. 5d – Fig. 5f). The stress concentration began to decrease on the back plate but the projectile force was still capable of

pushing the back plate (Fig. 5e) and projectile stopped  $v=0$  (Fig. 5f).

The plate configuration holds the projectile rate, so the projectile velocity gradually decreases. Initial velocity of the projectile was 989 m/s; in seconds, it gradually decreased to  $3.0006 \times 10^{-6}$  capable of being reduced to 975.55 m/s (Fig. 5a). The decrease of the projectile velocity when passing through the front plate was not significant (Fig. 5b-5d). However, the projectile velocity decreased significantly from second to second at  $2.7003 \times 10^{-5}$  to 303.24 m/s after the projectile end touched the back plate (Fig. 5e). The projectile stopped  $v=0$  the seconds to  $8.76 \times 10^{-5}$ . The back plate stopped the projectiles rate after penetrating the front plate. Seen in back plate, equivalent stress has not reached the maximum, so the back plate was capable of stopping the projectiles.

The projectile with an ogival/tapered-nosed (Fig. 2a) was able to stab front plate which used low strength and high strain. This is indicated by the decrease in speed that occurred. However, the projectile was successfully stopped by the back plate despite using the same type of material.



This was due to between the first plate and the second plate there was a boundary or isolation concentration stress, so the voltage on the first plate was not directly transferred to the second plate. The formation of these petals is the same as has been reported in previous studies [20] [21].

In this S.0 sandwich plate configuration, both experiment and simulation, the projectile could penetrate the front plate. The simulation proved that manufacturing with sandwich form in this study was able to isolate stress concentration distribution. The maximum stress concentration that occurred in the first plate was not directly distributed to the second plate. Visible line limited the distribution of stress between the first plate and the second plate. This caused the back plate would never reach maximum stress concentration, so the back plate was a slightly failure. Therefore, the back plate was able to stop the projectile rate after the front plate absorbed the impact force of the projectile. This simulation also showed and proved the deformation process on the plate to form petal.

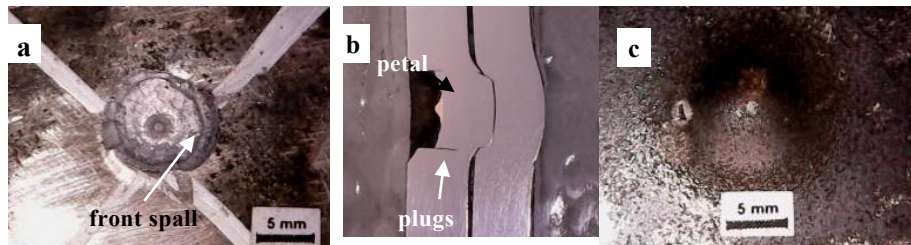


Fig. 6. Ballistic impact on the H.0 configuration (a) front face in front plate, (b) cross section and (c) rear face in back plate

Furthermore, in the H.0 configuration, the petals on the front face were not found. Hard material with high strength and low strain tended to be brittle. The projectiles couldn't pierce the plate. High velocity projectiles caused fractures around the crater lip and then broken plate formed a cylinder plugging. Plugging mechanism occurred because the end of projectile was blunt due to impact. Projectile caused failure by plugging which involved shearing by hemispherical-nosed projectiles [9]. This plugging shape was formed in high strength armor steel 10 mm of thickness impacted by 7.62 mm deformable projectiles [22]. Real perforation did not appear in this configuration because the cylinder plugging was restrained by the back plate. H.0 configuration (high strength, low strain) would significantly become more superior ballistic resistance than the S.0 configuration because of its resistance that was capable of breaking the tip of the projectile. It has also been submitted by Borvik et al. [23], where the high strength and low ductility material was ArmoX 560T of the upper layer, while the low strength and high ductility material was Weldox 700E to be used against blunt-nosed projectile and in Yunfei et al., [7] the target plates were made of 45 steel and Q235 steel to be used against blunt and ogival-nosed projectile.

The simulation in H.0 sandwich plate configuration is presented in Fig. 7. As has been done in the experiment, projectiles were not able to penetrate the front plate. The front plate using a hard plate retained the pointed end of the projectile. The projectile crushed on the front plate, so the projectile was unable to further penetrate the configuration. In the beginning, the tip of the projectile was able to deform the front plate (Fig. 7a). Maximum stress that occurred at the front plate was represented by

### 3.2. Hard plate – soft plate (H.0)

The H.0 sandwich plate configuration used hard plate as front plate and soft plate as back plate. In this configuration, after ballistic test, the projectile was able to break front plate but did not completely perforate. Impacts from ballistics in this configuration was different from S.0 configuration. Ballistic impact in H.0 configuration see Fig. 6. The front plate looked slight deformation. The front face looked spalls on the crater lip and the projectile scraps attached (Fig. 6a). The front plate was broken, and it formed cylinder plugging with small petal inside (Fig. 6b). Cylinder plugging pushed the back plate due to formed smooth bulge at rear face in back plate (Fig. 6c). Front plate used from hard plate was able to reach the projectile tip. High hardness and high strength plate was able to resist the velocity. Failure model of the front plate in H.0 configuration was plugging which spall in lips crater on front face. Plugging and spall formed wherefore plate was difficult to deform. As the result, front plate was cut/broken due to the high shear stress of the projectile impact.

the red color. Maximum stress was not distributed directly to the back plate; this was indicated by the absence of red color in the back plate. Although, the stress caused by the projectile impact was very large. However, because the front plate had high strength, the projectile tip began to deform (Fig 7b). In this case, the maximum stress in the plate didn't occur as indicated by the absence of red color on a plate (Fig. 7b). Projectile increasingly deformed, and the stress concentration was distributed to the back plate (Fig. 7c and Fig 7d). The projectile failed and was unable to penetrate the configuration (Fig. 7d and Fig. 7e). Finally, the projectile was capable of being stopped by configuration and the maximum stress didn't occur in the plate (Fig. 7f).

The projectile velocity gradually decreased after hitting the plate. The decrease of projectile velocity at the second to  $3.0006 \times 10^{-6}$  s was 964.95 m/s (Fig. 7a). The projectile velocity dropped significantly in seconds to  $2.101e \times 10^{-5}$  to 382.01 m/s (Fig. 7c). Projectile was able to be stopped ( $v=0$ ) on second to  $5.57 \times 10^{-5}$  (Fig. 7f) and the projectile broke and reversed. In this configuration, the front plate using a material with high strength and low strain was able to collect the projectile tip and thwart the projectile. Although, the projectile was able to break the plate but the projectile was unable to puncture the front plate. The impact force of the projectile results in maximum stress that was 1901.6 MPa which occurred in seconds to  $2.101e \times 10^{-5}$  s (Fig. 7d), and after that the maximum stress gradually decreased.

As the S.0 configuration, the sandwich plate in H.0 configuration could isolate the stress distribution. The maximum stress concentration occurring on the first plate was not entirely distributed to the second plate (Fig 5 and

Fig 7). This indicated that there was no maximum stress that occurred in back plate. Visible boundary line stress concentration of real between front plate and back plate.

Therefore, the back plate never occurred maximum stress concentration, consequently back plate slightly failed.

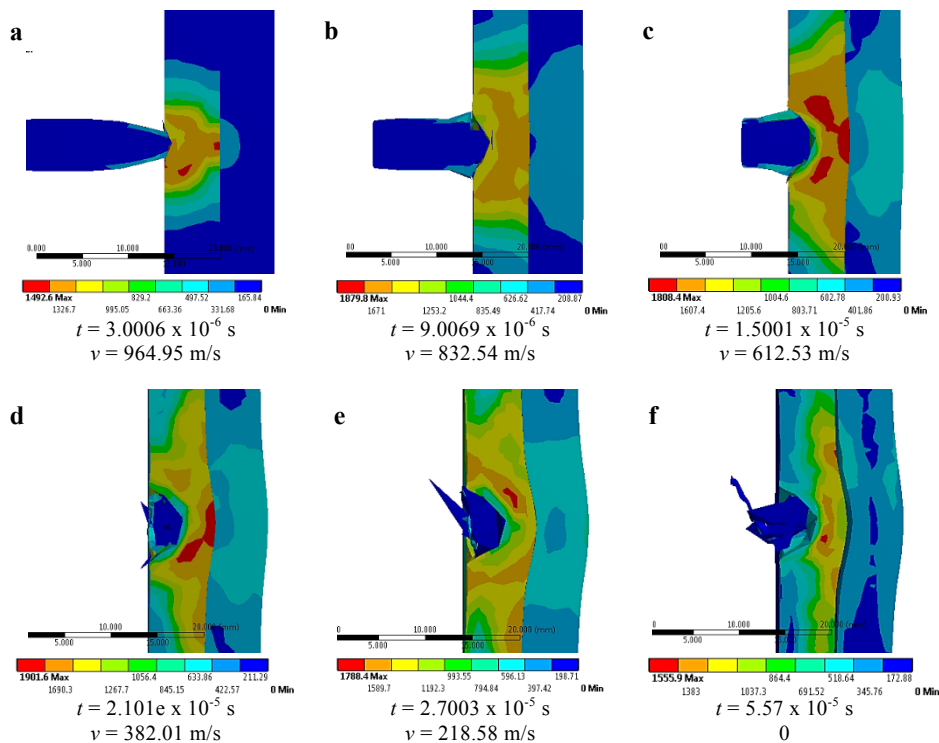


Fig. 7. Impact process of projectile on plate H.0 configuration (equivalent stress-von misses)

The difference in hardness material of the front plate in S.0 and H.0 configuration caused ballistic impact and different stress concentrations. In S.0 configuration, it appeared petal on hole lip because soft plate was made of easily deformed plastic. While the H.0 configuration lead the broken plate on the hole lip because the material was hard and brittle. In S.0 configuration, shortly after the projectile tip of the front plate reached the maximum stress, the next second the projectile could puncture the front plate. While at H.0, the maximum stress concentrations occurred in seconds to  $1.5001 \times 10^{-5}$  and occurred in a small area. This caused the S.0 configuration projectile got more penetrations. The decrease of projectile velocity in H.0 configuration was earlier than in S.0 configuration. In H.0 configuration, projectile velocity decreased in seconds to  $2.101 \times 10^{-5}$ . While in S.0 configuration was on second  $2.7003 \times 10^{-5}$ . Therefore, in H.0 configuration, projectile

could be stopped earlier i.e. at second to  $5.57 \times 10^{-5}$ . While in S.0 configuration, projectile stopped at second to  $8.76 \times 10^{-5}$ . Front plate failures were in both configurations; failure of soft material was due to deformation whereas in the hard material the failure was due to broken and forming a plug.

### 3.3. Soft plate – rubber – soft plate (S.2, S.4 and S.6)

The results of ballistic impact at S.2 sandwich plate configuration see Fig 8; S.4 configuration is in Fig. 9 and S.6 configuration is in Fig. 10. The ballistic effects generated in each of these configurations are similar to S.0 sandwich plate configuration. The use of soft plates on the front plate results in a petalling failure model due to deformation.

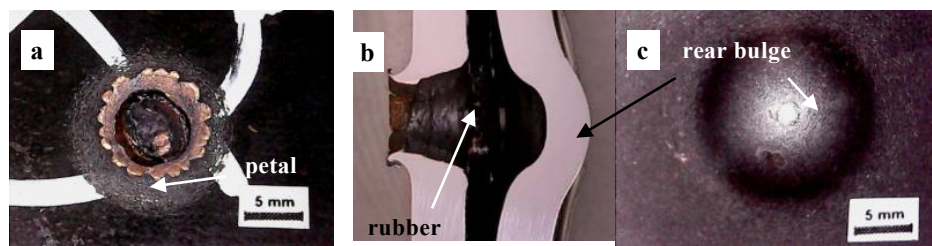


Fig. 8. Ballistic impact in the S.2 configuration (a) front face in front plate, (b) cross section and (c) rear face in back plate

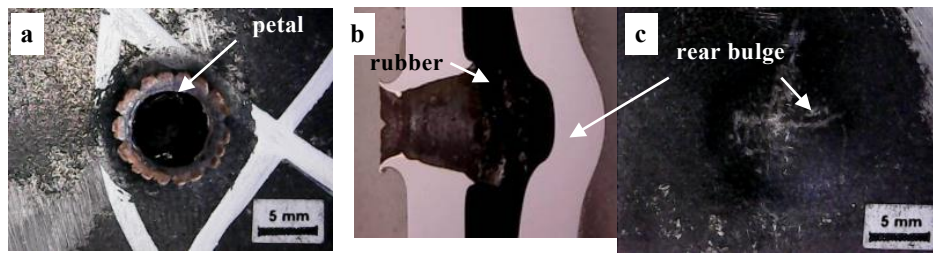


Fig. 9. Ballistic impact in the S.4 configuration (a) front face in front plate, (b) cross section and (c) rear face in back plate

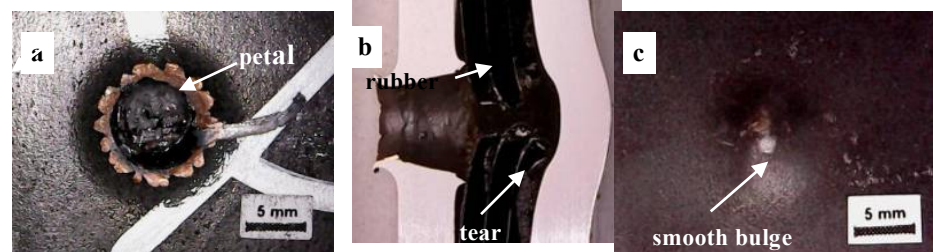


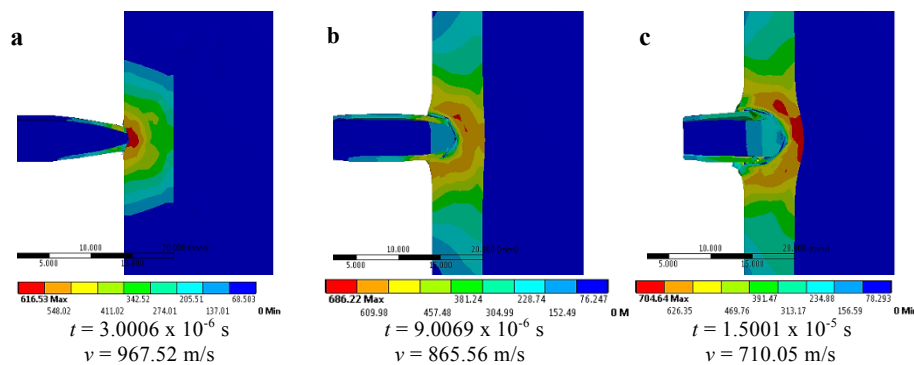
Fig. 10. Ballistic impact in the S.6 configuration (a) front face in front plate, (b) cross section and (c) rear face in back plate

Rubber layer addition in configurations forming sandwich soft plate – rubber – soft each with a thickness of rubber 2, 4 and 6 mm, front plate couldn't resist to ballistic impact. Front plate could penetrate the projectile with a similar mechanism in the S.0 configuration without rubber. Petal was formed in the front face indicating material was ductile (Fig. 8a, Fig. 9a and Fig. 10a). Projectile penetration and a plastic deformation occurred in the plate, so that the crater diameter formed was larger than the projectile diameter. The projectile was also capable of tearing the rubber after penetrating the front plate (Fig. 8b, Fig. 9b and Fig. 10b). The impact of the projectile and spall created basin on the inside and the bulge on the rear face configuration (Fig. 8c, Fig. 9c and Fig. 10c). Spall occurred on the inner side and tore out the rubber to hit the back plate.

Petal formations in the front face were similar to S.0 configuration without the rubber layer addition. The projectile tip was capable of piercing and deforming because the plate had a low strength and high strain. The layer addition of rubber was not able to absorb the impact energy of a high velocity of projectile. The layer addition of rubber in S.0 configuration did not significantly influence the ballistic impact. This was similar to the spaced multi-layered targets with small air gap as Yunfei et

al. [9] did, where the air gap had slight influence on the ballistic resistance. While Wei et al. [13] declared the layered targets with larger air gap were stronger than those with small air gap. Rubber layer addition in sandwich was only able to absorb and degrade projectile velocity to back plate.

An example of the simulation in the sandwich plate configuration with the layer addition of rubber was given to a rubber thickness of 6 mm. The projectile penetration and stress distribution process occurring in the S.6 configuration are shown in Figure 11. The projectile could penetrate the front plate because the maximum stress that occurred exceeded the tensile strength of the material. This could be seen from the stress concentration of the red color (616.53 MPa) in the front plate immediately the tip of the projectile impact (Fig. 11a). Projectile pierced the front plate (Fig. 11b) and a projectile began to deform (Fig. 11c). The stress concentration in the front plate began to be distributed to the back plate through the rubber, and the maximum voltage in this configuration occurred i.e. 721.43 MPa (Fig. 11d). Stress concentration caused by the ballistic impact was still high, so that the front plate was failure (Fig 11e). The projectile successfully penetrated the front plate and rubber, so that it hit of the back plate (Fig. 11f and Fig. 11g).





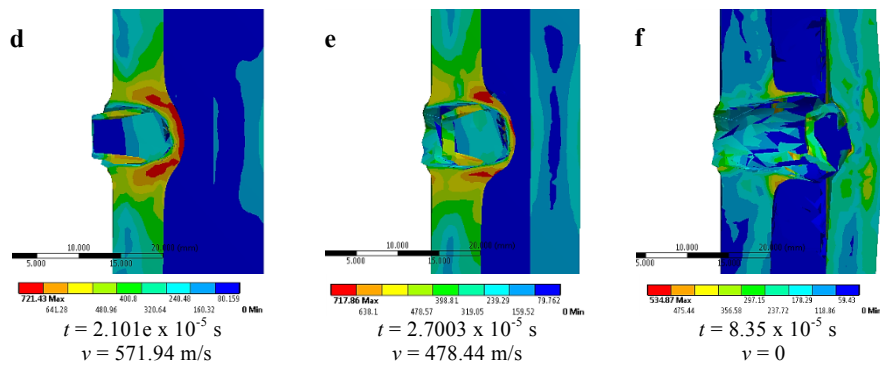


Fig. 11. Impact process of projectile in plate S.6 configuration(equivalent stress-von misses)

Similar to the configuration without rubber in the soft plate, stress concentration distributions could be isolated by sandwich manufacturing. The stress that occurred on the front plate was not directly transferred to the back plate. With the layer additional rubber, stress concentration resented to distributed to the back plat at the second to  $2.101e \times 10^{-5}$ . The projectile velocity dropped to 478.44 m/s at the end of the front plate and began to penetrate the rubber. The projectile stopped ( $v=0$ ) at second to  $8.35 \times 10^{-5}$  after projectile held back plate and projectile was destroyed. The layer addition of rubber experimentally did not show any difference, but the simulation analysis shows the difference of stress concentration distribution shown by the difference of color as indicator of equal equivalent stress.

With mere experiments, it is difficult to see the difference of impact projectile effect on the configuration

without rubber and with rubber. However, the simulation can measure and view the maximum voltage occurred. With the layer addition of rubber to all S configurations (front plate with soft plate), the stress occurred relatively smaller. In the configuration without rubber, maximum stress occurred was 1027.6 MPa. While the configuration with the layer addition 6 mm rubber of thickness, maximum stress occurred was 721.43 MPa.

### 3.4. Hard plate – rubber - soft plate (S.2, S.4 and S.6)

The results of ballistic impact in the H.2 sandwich plate configuration see in Fig. 12, H.4 configuration is in Fig. 13, and H.6 configuration is in Fig. 14.

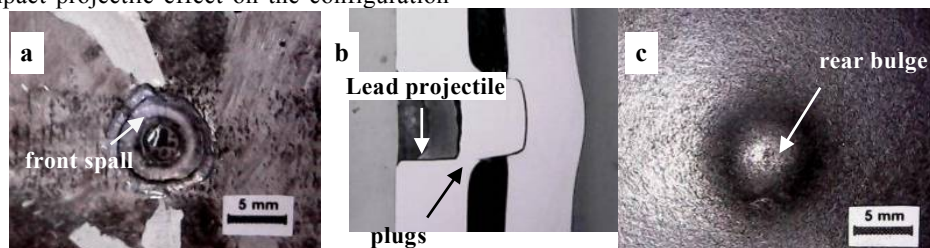


Fig. 12. Ballistic impact on the H.2 configuration (a) front face in front plate, (b) cross section and (c) rear face in back plate

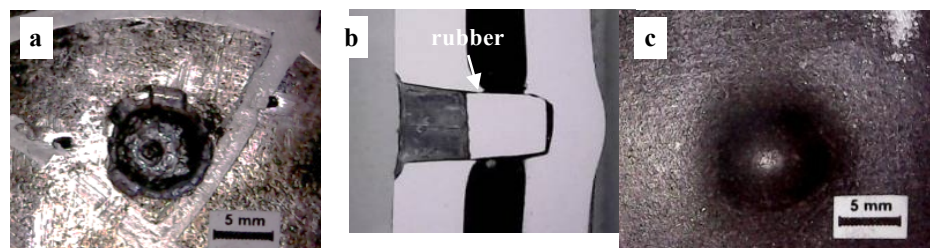


Fig. 13. Ballistic impact on the H.4 configuration (a) front face in front plate, (b) cross section and (c) rear face in back plate

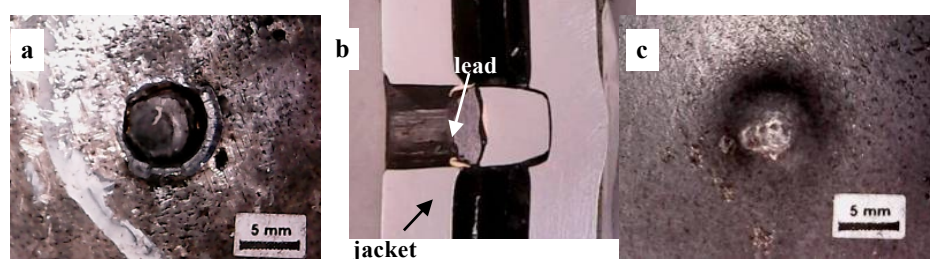


Fig. 14. Ballistic impact on the H.6 configuration (a) front face in front plate, (b) cross section and (c) rear face in back plate

The layer addition of rubber between the plates in H.2, H.4 and H.6 did not significantly influence the ballistic characteristics such as the H.0 configuration without rubber. Projectile was able to break the front plate, thus formed the spall around the crater lip (Fig 12a, Fig 13a and

Fig 14a). Plugging that was formed tore out and penetrated the rubber (Fig 12b, Fig 13b and Fig 14b). Plugging that was formed also hit the back plate to form a bulge on the rear face (Fig 12c, Fig 13c and Fig 14c).



No petal formation in the front face due to hard materials and low strain, while plate tended to be brittle. The tip of projectile was not capable of piercing the plate, while a projectile with ogival/taper-nose deforming was blunt after hitting the surface of the high strength plate. This was an evidence formed of the remaining lead of projectile in the crater. Macro observations showed there were no significant differences of each configuration in the rubber thickness on the hard plate samples. The layer addition of the rubber between the plates on the whole H configuration precisely caused the front plate to be pierced. This was due to the rubber was not able to hold the plug. Sarlin et al. [17] reported that steel/rubber/composite hybrid structure on the energy absorption and the damage behavior of the studied hybrid structure were rather immune to the changes in the test parameters, only attack angle showed a stronger effect.

The equivalent stress occurred in the H.6 configuration due to ballistic impact is presented in Fig. 15. The stress concentration that occurred in the configuration in hard plate with the layer addition of rubber was similar to the

configuration in hard plate without rubber. On the H.6 configuration, maximum stress concentration also occurs only on the front plate. The front plate failed due to the equivalent stress that occurred exceeded the strength of the material. Projectile also experienced maximum stress, so that deformed from seconds to  $9.0069 \times 10^{-6}$  (Fig. 15b). However, because of the large impact force of the projectile, the projectile was capable of perforating the front plate. Projectile impact was also able to tear the rubber (Fig. 15d). But with the layer addition of the rubber in all H configurations, the average equivalent stress that occurred was relatively lower than the without of rubber (Fig. 7). Without rubber, maximum stress that occurred in the plate was 1901.6 MPa (Fig. 7d). While the configuration with the layer addition 6 mm rubber of thickness, maximum stress that occurred was 1016.0 MPa (Fig 7d). Equivalent stress average which appeared in the simulated results showed that the thicker of the rubber layer showed a smaller equivalent stress, this was indicated by the color difference as an indicator [13].

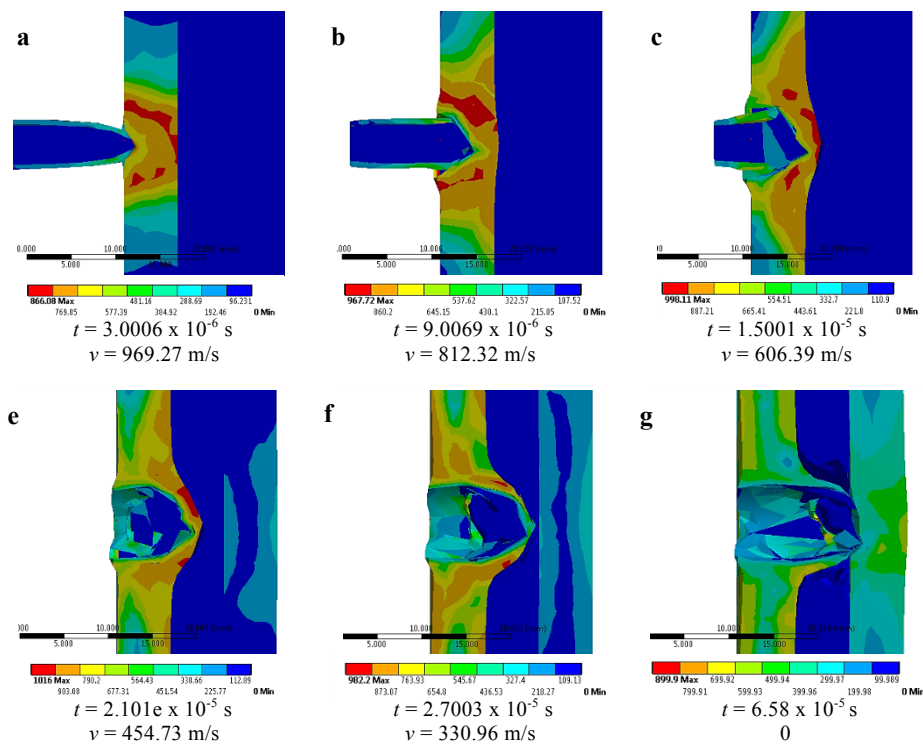


Fig. 15. Impact process of projectile on plate S.6 configuration (equivalent stress-von misses)

The simulation results in all configurations show that the manufacturer of sandwich plate gives the distribution of maximum stress concentrations only in the first plate. The maximum stress that occurred in the first plate is not directly transferred to the next layer. Therefore, the next layer does not experience the maximum stress. This causes the second plate (back plate) does not fail as the first plate (front plate). The layer addition of rubber to each configuration can lower the maximum stress that occurs in the plate.

### 3.5. i

The effect of projectile impact in the plate of the experimental test (*Ex*) and simulations (*S*) was measured for analysis. Measurements include depth of penetration (*DoP*), petal high (*p*), crater diameter (*d*), and bulge high (*d*). Measurement result in the experimental test and the

simulation in each configuration showed similarity trends. Dimensional measurement results to the ballistic impacts in every configuration plate is shown in the chart of Fig. 16.

The measurements of depth of penetration (*DoP*) in the front plate (*DoP I*) and the back plate (*DoP II*) are shown in Fig. 16a. *DoP I* in the all S configurations cannot be measured, because the front plate was perforated by a projectile. *DoP I* in the all H configurations, increase of thickness the rubber layer between the plates, the depth of penetration is deeper. This was due to the rubber between the plates was torn by the plugs, so that the thicker rubber increasingly provided space of the plugs to be pushed. *DoP II* in the all S configurations showed that the thicker the rubber the lower the penetration depth. This was due to the failure model in S configuration was fragmentation, while

front plate fractures are small pieces of flake that spread between plates. Therefore, the fragments that impacted the energy were not concentrated in one area of penetration so that the depth of penetration in the back plate became smaller. Projectile and plate fractures were spread between the rubber and the plate in the all S configurations as shown in Fig. 17. The presence of flakes found between these layers also proved that failure model in S

configuration was fragmentations. *DoP II* on all H configurations, the layer addition of rubber did not affect the different depth of penetration in the back plate. Due to the front plate was better able to withstand projectiles and failure model in this configuration was plugging (Fig 6, 12, 13 and 14). Plug slightly push back plate and stuck by the layer addition of rubber.

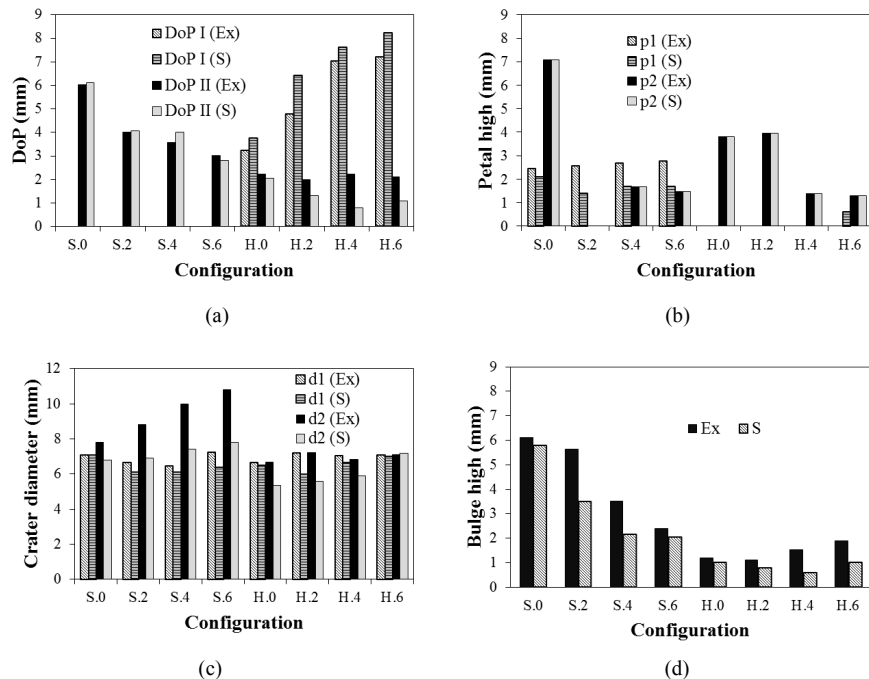


Fig. 16. Dimensional ballistic impacts in every configuration (a) depth of penetration, (b) petal high, (c) crater diameter and (d) bulge high

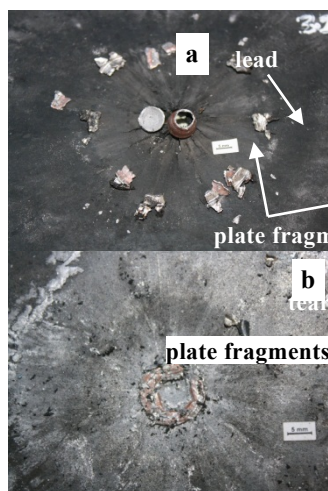


Fig. 17. Fragments of front plate and projectile (a) in the rubber (b) in the back plate

Graph of petal height ( $p$ ) formed is see Fig. 16b. Petal in the front face in the S configuration was due to the high deformation plate. Plate with high strain will form the petal and petalling is produced by high radial and circumferential tensile stresses after passage of the initial stress wave [24]. The petals formed in the front face S configuration indicated the thicker the rubber, the petals formed was also higher although it was not significant. It was a little proves that the layer addition of rubber could increase the ability of deformation and this needs to be further studied. While on the inner side of front plate either in the all S configurations or all H configurations indicated that a petal height was irregular.

The diameter of the crater ( $d$ ) caused by the ballistic impact of each configuration is shown in Figure 16c. Crater diameter in the all S configuration was larger than the projectile diameter used i.e. 5.56 mm, as reported Hub and Komenda [14]. The average crater diameter of the front face ( $d_1$ ) all S configuration was 6.86 mm and the front inner plate ( $d_2$ ) was 9.36 mm. This was due to the plate with the low strength and high strain occurred lateral plastic deformed the projectiles direction. Furthermore, the inner front plate, besides lateral deformation, the plate also suffered fractures, proved by the residual fracture as shown in Figure 17. Jena et al. [22] also stated that ductile hole was clearly seen from their crater halves and the diameter of the hole was bigger than the actual projectile diameter. Therefore, failure in this case was caused by ductile hole growth [24] or ductile hole formation [25]. While the crater diameter in the all H configuration was relatively the same between the front face and the inner front plate, this occurred due to the fracture mechanism of the plugging. The average crater diameter was 7.01 mm on the front face and 6.96 mm on the inner front plate. The crater diameter was also larger than the diameter of the projectile used. This was due to end of the projectile impact the plate with high strength, projectile occurred lateral deformed, that the projectile was deformed and ruptured so projectile a mass reduction.

Graph of High bulges ( $B$ ) in the rear face formed by residual energy at the back plate in each configuration is shown in Fig. 16d. In the all S configurations, the layer addition of the rubber thickness got smaller bulges height, but H configuration the layer addition of rubber thickness actually increased the bulge height, although it was not significant. In the all S configurations, fracture occurred was a small fracture that spread so the layer addition of

rubber was capable of absorbing residual energy of the plate and projectile fracture. While the H configuration, a fracture in the singular and rubber was not able to absorb residual energy to encourage the back plates to form a bulge.

#### 4. Conclusions

Study on the effect of soft - hard plate and rubber thickness as absorbent impact to the ballistic resistance with 5.56 x 45 mm caliber deformable projectile has been done by experiment and numerical simulation. The following conclusions are drawn:

1. The hardness, tensile strength, strain and impact energy influence the crater characteristics plate sandwich resulting in deformable projectile impact.
2. The plate configuration with low hardness, low strength and high strain as the front plate in a sandwich front plate - rubber - back plate produces ballistic impacts with petalling mechanism due to lateral deformation and fragmentation mechanism. Therefore, it appears that the petals are high and the crater diameter are larger than the projectile used. The fragments push back plate to form a bulge on the rear side.
3. The plate configuration with high hardness, high strength and low strain as the front plate in a sandwich front plate-rubber-back plate produces ballistic impacts with plugging mechanism due to end of projectile into a blunt of so as to form a cylinder plug and shear formed crater. The plug pushes back plate forming a bulge on the rear side.
4. Using the simulation, the stress concentration behavior caused by the impact projectile can be shown that the maximum stress concentration occurs only on the front plate, so the front plate failure.
5. The configuration of hard plate as front plate reveals minimum ballistic impact due to the projectile rate. It is indicated on the impact of the damage, stress distribution and time of the projectile after the plate configurations.

#### Acknowledgement

Thank to the Ministry of Research Tecnology and Higher Education Republic of Indonesia for the grant doctoral research no: 025/K6/SP2H/PENELITIAN/2017.

This is an Open Access article distributed under the terms of the Creative Commons Attribution License



#### References

1. V. R. Aparow, K. Hudha, M. M. Hamdan, and S. Abdullah, Study on Dynamic Performance of Armoured Vehicle in Lateral Direction due to Firing Impact., *Adv. Mil. Technol.* **10** (2015).
2. T. B. Bhat, Science of armour materials, *Def. Sci. J.* **35**, 219–223 (2014).
3. J. A. Zukas and D. R. Schefflerb, Impact Effects in Multilayered Plates, *Int. J. Solids Struct.* **38**, 3321–3328 (2001).
4. W. Liu, Z. Chen, X. Cheng, Y. Wang, A. R. Amankwa, and J. Xu, “esign and ballistic penetration of the ceramic composite armor, *Compos. Part B Eng.* **84**, 33–40 (2016).
5. V. Sháněl and M. Španiel, Ballistic Impact Experiments and Modelling of Sandwich Armor for Numerical Simulations, *Procedia Eng.* **79**, 230–237 (2014).
6. S. Dey, T. Børvik, X. Teng, T. Wierzbicki, and O. S. Hopperstad, On the ballistic resistance of double-layered steel plates: An experimental and numerical investigation, *Int. J. Solids Struct.* **44**, 6701–6723 (2007).
7. D. Yunfei, Z. Wei, Y. Yonggang, S. Lizhong, and W. gang, Experimental investigation on the ballistic performance of double-layered plates subjected to impact by projectile of high strength, *Int. J. Impact Eng.* **70**, 38–49 (2014).
8. D. Yunfei, Z. Wei, Y. Yonggang, and W. Gang, The ballistic performance of metal plates subjected to impact by projectiles of different strength, *Mater. Des.* **58**, 305–315 (2014).
9. Y. Deng, W. Zhang, and Z. Cao, Experimental investigation on the ballistic resistance of monolithic and multi-layered plates against hemispherical-nosed projectiles impact, *Mater. Des.* **41**, 266–281 (2012).
10. X. Teng, S. Dey, T. Børvik, and T. Wierzbicki, Protection performance of double-layered metal shields against projectile impact, *J. Mech. Mater. Struct.* **2**, 1309–1329 (2007).
11. X. Teng, T. Wierzbicki, and M. Huang, Ballistic resistance of double-layered armor plates, *Int. J. Impact Eng.* **35**, 870–884 (2008).
12. P. Pěchouček, S. Rolc, and J. Buchar, Fragment Simulating Projectile Penetration into Layered Targets, *Eng. Mech.* **18**, 353–361 (2011).
13. Z. Wei, D. Yunfei, C. Z. Sheng, and W. Gang, Experimental investigation on the ballistic performance of monolithic and layered metal plates subjected to impact by blunt rigid projectiles, *Int. J. Impact Eng.* **49**, 115–129 (2012).
14. J. Hub and J. Komenda, Ballistic Resistance of Steel Plate Hardox upon Impact of Non-Penetrating Projectiles, *Adv. Mil. Technol.* **4**, 79–91 (2009).
15. C. Kaynak, A. N. Arikan, and T. Tincer, Flexibility Improvement of Short Glass fiber Reinforced Epoxy By Using A Liquid Elastomer, *Polymer* **44**, 2433.
16. D. Mohotti, T. Ngo, P. Mendis, and S. N. Raman, Polyurea coated composite aluminium plates subjected to high velocity projectile impact, *Mater. Des.* **52**, 1–16 (2013).
17. E. Sarlin, M. Lindroos, M. Apostol, V.-T. Kuokkala, J. Vuorinen, T. Lepistö, and M. Vippola, The effect of test parameters on the impact resistance of a stainless steel/rubber/composite hybrid structure, *Compos. Struct.* **113**, 469–475 (2014).
18. C. M. Roland, D. Fragiadakis, and R. M. Gamache, Elastomer–steel laminate armor, *Compos. Struct.* **92**, 1059–1064 (2010).
19. C. M. Roland, D. Fragiadakis, R. M. Gamache, and R. Casalini, Factors influencing the ballistic impact resistance of elastomer-coated metal substrates, *Philos. Mag.* **93**, 468–477 (2013).
20. B. Mishra, P. K. Jena, B. Ramakrishna, V. Madhu, T. B. Bhat, and N. K. Gupta, Effect of tempering temperature, plate thickness and presence of holes on ballistic impact behavior and ASB formation of a high strength steel, *Int. J. Impact Eng.* **44**, 17–28 (2012).
21. M. A. Iqbal, K. Senthil, P. Bhargava, and N. K. Gupta, The characterization and ballistic evaluation of mild steel, *Int. J. Impact Eng.* **78**, 98–113 (2016).
22. P. K. Jena, B. Mishra, K. Siva Kumar, and T. B. Bhat, An experimental study on the ballistic impact behavior of some metallic armour materials against 7.62mm deformable projectile, *Mater. Des.* **31**, 3308–3316 (2010).
23. Børvik, Hopperstad, Langseth, and Malo, Effect of target thickness in blunt projectile penetration of Weldox 460 E steel plates, *Int. J. Impact Eng.* **28**, 413–464 .
24. J. A. Zukas, Impact dynamics: theory and experiment, DTIC Document, 1980.(2000)
25. S. Karagoz, H. Atapek, and A. Yimaz, A fractographical study on boron added armor steel developed by alloying and heat treatment to understand its ballistic performance, 27 May 2008, Cairo, Egypt.